

***c*-Axis Optical Sum Rule and a Possible New Collective Mode in $\text{La}_{2-x}\text{Sr}_x\text{CuO}_4$** A. B. Kuzmenko,¹ N. Tombros,¹ H. J. A. Molegraaf,¹ M. Grüninger,² D. van der Marel,¹ and S. Uchida³¹*Material Science Center, University of Groningen, Nijenborgh 4, 9747AG, Groningen, The Netherlands*²*II Physical Institute, University of Cologne, 50937 Cologne, Germany*³*Department of Superconductivity, University of Tokyo, Bunkyo-ku, Tokyo 113, Japan*

(Received 19 February 2003; published 18 July 2003)

We present the *c*-axis optical conductivity $\sigma_{1c}(\omega, T)$ of underdoped ($x = 0.12$) and optimally doped ($x = 0.15$) $\text{La}_{2-x}\text{Sr}_x\text{CuO}_4$ from 4 meV to 1.8 eV obtained by a combination of reflectivity and transmission spectra. In addition to the opening of the superconducting gap, we observe an *increase* of conductivity above the gap up to 270 meV with a maximal effect at about 120 meV. This may indicate a new collective mode at a surprisingly large energy scale. The Ferrell-Glover-Tinkham sum rule is violated for both doping levels. Although the relative value of the violation is much larger for the underdoped sample, the absolute increase of the low-frequency spectral weight, including that of the condensate, is higher in the optimally doped regime. Our results resemble in many respects the observations in $\text{YBa}_2\text{Cu}_3\text{O}_{7-\delta}$.

DOI: 10.1103/PhysRevLett.91.037004

PACS numbers: 74.72.-h, 74.25.Gz, 78.20.Ci

The charge transport between the CuO_2 planes in the high- T_c cuprates forms one of the most intriguing puzzles of these materials. On the one hand the essential common physics seems to lie in the collective behavior of holes doped into a 2D Mott insulator, while the interplane conductivity strongly depends on the varying interlayer chemistry. On the other hand, it is the in-plane “confinement” that preserves a possibility of significant lowering of the *c*-axis kinetic energy (KE) as the 3D coherent movement of the Cooper pairs sets in below T_c [1,2]. This, however, was shown to be a small effect in some single-layer compounds [3,4]. The models based on the KE lowering in the superconducting (SC) state predict the violation of the Ferrell-Glover-Tinkham (FGT) optical sum rule [5], which means that the spectral weight (SW) of the SC condensate partly stems from energies much higher than 2Δ . In the *c*-axis data of $\text{YBa}_2\text{Cu}_3\text{O}_{7-\delta}$ (YBCO) a significant increase of the relative violation value was found in the underdoped regime [6]. In the case of $\text{La}_{2-x}\text{Sr}_x\text{CuO}_4$ (LSCO) a value of 50% has been reported for a slightly underdoped sample [7], although the doping dependence is still not known. Thus, the *c*-axis KE lowers in the SC state, which, however, leaves room for debate whether this is a by-product or the very reason for superconductivity [1,2,8,9].

The conclusiveness of the sum-rule analysis greatly depends on a reliable value of $\sigma_1(\omega, T)$. However, the usually employed Kramers-Kronig (KK) analysis of reflectivity seriously lacks accuracy due to the insensitivity of reflection to small absorption values and an ambiguity of the data extrapolation. This is a major problem for LSCO with a relatively small *c*-axis electronic conductivity [10]. In this Letter we report on our optical study of underdoped (UD) and optimally doped (OD) LSCO by a combination of reflection and transmission spectroscopy, which provides details of the redistribution of spectral weight due to the superconducting transition. We find out

that the increase of the total low-frequency SW (including condensate) below T_c can be at least partly explained by a new collective mode, which gives rise to a peak at 120 meV. Understanding this mode is essential in order to rate the relevance of the *c*-axis kinetic energy saving (which turns out to be higher in the OD regime) for the high- T_c mechanism.

The $\text{La}_{2-x}\text{Sr}_x\text{CuO}_4$ single crystals ($x = 0.12$, $T_c = 29$ K and $x = 0.15$, $T_c = 37$ K) were grown by the same method as described in Ref. [11]. The *c* axis was within 1° in the ac sample surface, as determined by Laue diffraction. Initially the reflectivity (R) spectra ($15\text{--}6000\text{ cm}^{-1}$) were obtained using a Fourier-transform spectrometer on thick samples with the surface area of $20\text{--}25\text{ mm}^2$ mounted on a copper cone [see Fig. 1(a)]. We used *in situ* gold evaporation as a reference. The spectra match very well with the previous data [10], which were used to continue curves to higher frequencies. Then each sample was attached to a supporting plane and reduced to a thin platelet by slow polishing with diamond paper with a roughness down to $0.1\text{ }\mu\text{m}$. The platelets were made 23 and $14\text{ }\mu\text{m}$ thick with areas of 1.3 and 1.0 mm^2 for $x = 0.12$ and 0.15 , correspondingly. Finally, the samples were unglued from the support and mounted on a copper mask. The *c*-axis transmission (T) spectra [see Fig. 1(b)] have been measured using a Fourier-transform spectrometer ($20\text{--}6000\text{ cm}^{-1}$) and a grating-type spectrometer ($6000\text{--}15\,000\text{ cm}^{-1}$). At higher frequencies the samples are not transparent presumably due to the charge-transfer absorption, at lower energies the diffraction effects mask the data. We used freestanding thin crystals to avoid complications due to a substrate. The transmission for $\mathbf{E}\parallel\mathbf{a}$ was immeasurably small, indicating the absence of any “pinhole” leakage. All the measurements were done in a homemade optical cryostat with a temperature-stable sample position. The absolute systematic error bars of R and T are about 0.01

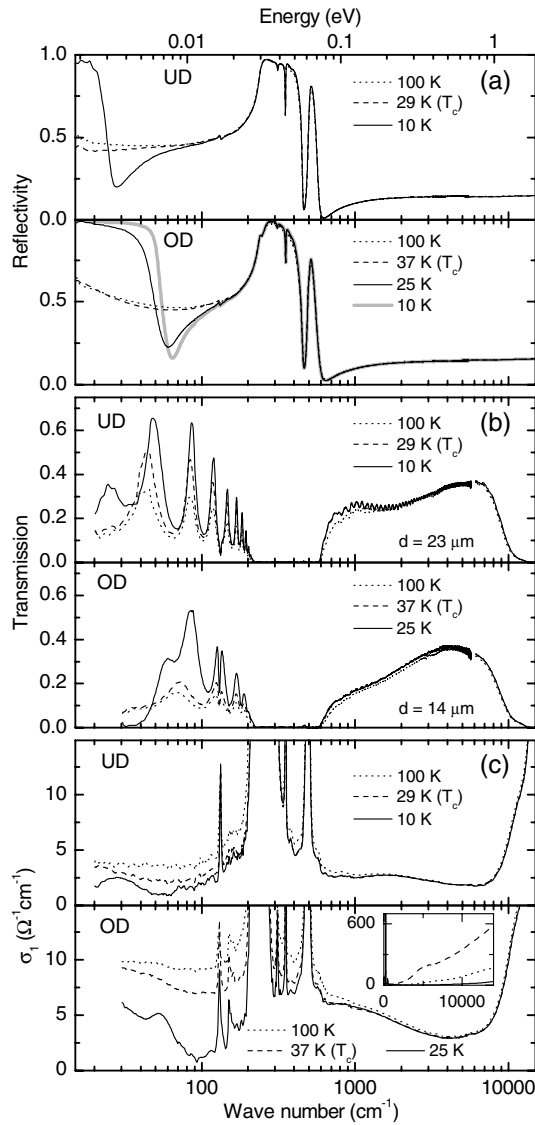


FIG. 1. The c -axis reflectivity (a), transmission (b), and optical conductivity (c) of the UD ($x = 0.12$) and the OD ($x = 0.15$) LSCO samples. The inset compares $\sigma_1(\omega, 300 \text{ K})$ (solid line) with the previous results based on reflectivity data only (Ref. [12]: dashed line; Ref. [13]: dotted line).

and 0.03, respectively. The accuracy of their relative temperature difference is at least 1 order of magnitude better. We focus on the low-temperature data well below the structural phase transition (tetragonal to orthorhombic). The temperature precision is about 1 K [14].

The measured $R(\omega)$ and $T(\omega)$ are functions of $\epsilon(\omega) = \epsilon_1(\omega) + i\epsilon_2(\omega)$:

$$R = |r|^2, \quad T = \left| \frac{(1-r^2)t}{1-r^2t^2} \right|^2, \quad (1)$$

$$r = \frac{1 - \sqrt{\epsilon}}{1 + \sqrt{\epsilon}}, \quad t = e^{i(\omega/c)\sqrt{\epsilon}d},$$

where d is the sample thickness. These formulas can be applied to derive ϵ_1 and ϵ_2 from R and T (RT method) for

frequencies above 650 cm^{-1} and below 200 cm^{-1} without the use of the KK relations. In the phonon range, where T is vanishingly small, the KK transformation still should be exploited. Our combined approach (called “RT + KK”) is to find the best KK-compatible function $\epsilon(\omega)$, which matches experimental $R(\omega)$ and $T(\omega)$ simultaneously in the whole spectral range [15]. The sample thickness is determined by the period of Fabry-Pérot oscillations [16]. The optical conductivity $\sigma_1(\omega) = \omega\epsilon_2(\omega)/4\pi$ is shown in Fig. 1(c). Notably, above 1000 cm^{-1} σ_1 is significantly smaller than the previously published values based solely on reflectivity data [12,13] [see inset in Fig. 1(c)].

The temperature dependence of σ_1 is shown in Fig. 2(a). It is not constant above T_c , therefore the difference $\Delta\sigma_1 = \sigma_1(T = T_c) - \sigma_1(T \ll T_c)$ does not represent purely a superconductivity-induced change of $\sigma_1(\omega)$. Instead, we use the distinct *slope jump* at T_c ,

$$\Delta_s\sigma_1 \equiv (\partial\sigma_1/\partial T)|_{T_c+} - (\partial\sigma_1/\partial T)|_{T_c-}, \quad (2)$$

to characterize the effect of the SC transition. The negative value of $\Delta_s\sigma_1$ at low frequencies is indicative of the gap opening. However, it becomes *positive* at higher energies $\sim 1000 \text{ cm}^{-1}$ (120 meV) and disappears within the noise level above $\Omega_c \approx 2200 \text{ cm}^{-1}$ (270 meV). The “anomalous” kink at intermediate energies is nicely seen in the original transmission data, which we double-checked with an enhanced temperature resolution [Fig. 2(d)]. The decrease of T below T_c corresponds to an increase of σ_1 . The spectral weight of the condensate (δ function at $\omega=0$) $D(T)$ is shown in Fig. 2(c). We obtain

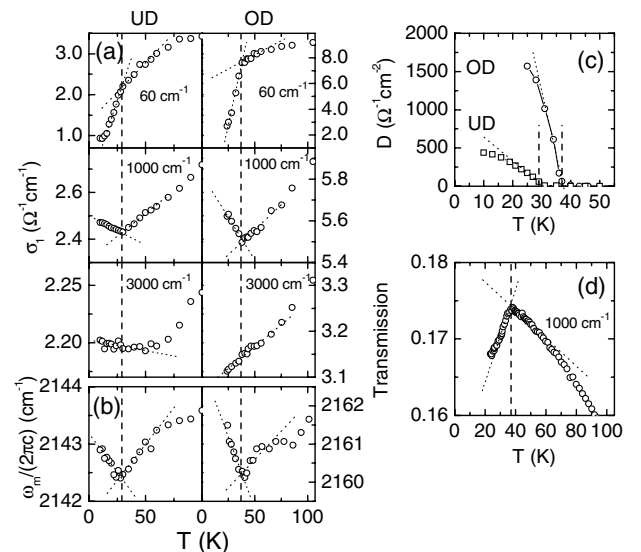


FIG. 2. The temperature dependence of (a) conductivity at selected energies, (b) a Fabry-Pérot maximum position at $\approx 2150 \text{ cm}^{-1}$, (c) the condensate SW, and (d) the transmission of the OD sample at 1000 cm^{-1} with a fine temperature resolution. The dotted lines denote the curve slopes above and below T_c , which is marked by the vertical line.

$\Delta_s D$ of 27 and $130 \Omega^{-1} \text{cm}^{-2} \text{K}^{-1}$ for UD and OD samples, respectively, which is also denoted by the hatched area in Fig. 3(a).

The spectral dependence of the conductivity kink is shown in Fig. 3(a). The most accurate value of $\Delta_s \sigma_1$ is obtained in regions of nonzero transmission. The error bars increase in the phonon range, especially near the very intense peak at 240 cm^{-1} , which complicates the sum-rule analysis. The difficulty can be circumvented by assuming a smooth shape of $\Delta_s \sigma_1(\omega)$ and fitting it with a function, which can be used to “bridge” the problematic frequency range. The model function $\Delta_s \epsilon = \Delta_s \epsilon_1 + i\Delta_s \epsilon_2$ has to satisfy the KK relations. In addition to $\Delta_s \sigma_1(\omega) = \Delta_s \epsilon_2(\omega)/4\pi$ below and above the phonons [Fig. 3(a)] we fit the experimentally observed spectrum of $\Delta_s R(\omega)$ inside the phonon region [Fig. 3(b)] using the relation

$$\Delta_s R = (\partial R/\partial \epsilon_1)\Delta_s \epsilon_1 + (\partial R/\partial \epsilon_2)\Delta_s \epsilon_2, \quad (3)$$

where the derivatives $\partial R/\partial \epsilon_{1,2}$ are obtained by the RT + KK method at T_c (the idea is similar to that of the temperature modulation technique). Important extra information on $\Delta_s \sigma_2$ (or $\Delta_s \epsilon_1$) is given by the Fabry-Pérot extrema positions ω_m [see Fig. 2(b)]. The product $\omega_m \sqrt{\epsilon_1} d$ is a constant (if $\epsilon_2 \ll \epsilon_1$); therefore,

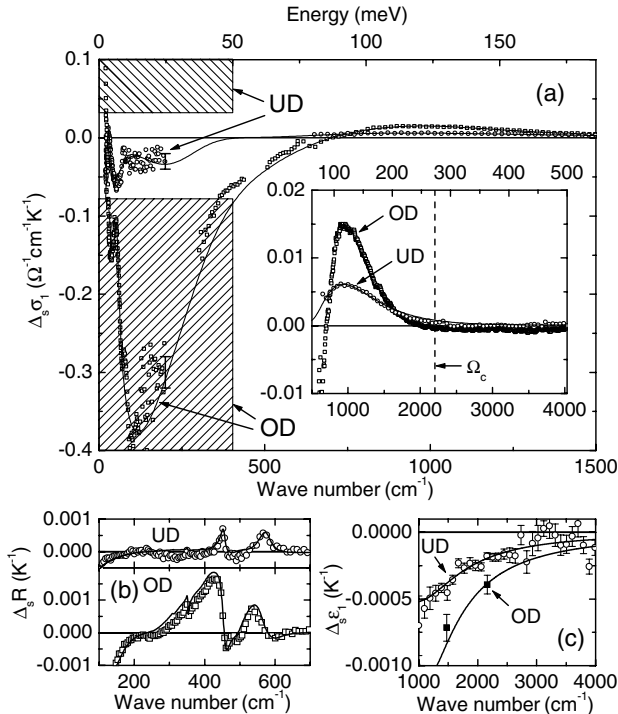


FIG. 3. (a) $\Delta_s \sigma_1(\omega)$ (the hatched area corresponds to the slope change of SW at $\omega = 0$, $\Delta_s D$), the error bars represent experimental uncertainty of $\Delta_s \sigma_1(\omega)$ below 200 cm^{-1} ; the inset expands the higher frequency region, where transmission allows a very accurate determination of $\sigma_1(\omega)$. (b) $\Delta_s R(\omega)$ in the phonon range. (c) $\Delta_s \epsilon_1(\omega)$ at high frequencies, as derived from the shift of Fabry-Pérot fringes. The solid curves represent the fit as described in the text.

037004-3

$$\Delta_s \epsilon_1 = -2\epsilon_1(\Delta_s \omega_m/\omega_m + \Delta_s d/d). \quad (4)$$

The c -axis lattice constant does not show a kink at T_c [17] so that the spectral dependence of $\Delta_s \epsilon_1$ can be directly determined from ω_m 's and fitted together with $\Delta_s \sigma_1$ and $\Delta_s R$ [see Fig. 3(c)]. The high-frequency $\Delta_s \epsilon_1$ is especially useful because it is related to the total low-frequency SW (including condensate) [18]

$$\Delta_s \epsilon_1(\omega) \approx -8\Delta_s[A(\Omega_c) + D]\omega^{-2}, \quad (5)$$

where $A(\omega) \equiv \int_{0+}^{\omega} \sigma_1(\omega') d\omega'$. We obtained a reasonably good fit of $\Delta_s \sigma_1$, $\Delta_s R$, and $\Delta_s \epsilon_1$ simultaneously (see Fig. 3), which is prerequisite for a reliable sum-rule examination.

The superconductivity-driven change of σ_1 below T_c (detectable for $\omega < \Omega_c$) is governed by two factors: (i) the SC gap opening and (ii) the increase of SW above the gap. The former is much more pronounced for the OD sample (~ 8 times larger effect). It is therefore remarkable that the latter is only 1.8–2 times smaller for the UD sample. In principle, a slight conductivity increase above the gap is expected in BCS theory in the clean limit. However, the incoherent c -axis transport is far in the dirty limit, especially in the UD regime, and calculations give a small size of this effect [19]. We propose that the observed increase of σ_1 is a signature of a new collective mode emerging (or sharpening) below T_c . The nature of this mode is not clear at the moment. Its energy scale (100–270 meV) is much higher than 2Δ (~ 20 – 30 meV [20]). The single-layer structure seems to exclude the transverse plasmon scenario put forward for YBCO [21,22]. However there is a similarity between the effect we observe in LSCO and the increase of conductivity at the same energies in YBCO [21–23], so that the possibility that the phenomena in these two compounds are common in origin cannot be ruled out, even though the value of σ_1 as well as its absolute change below T_c is much larger in YBCO.

The occurrence of several collective modes has been recently predicted by Lee and Nagaosa [24] from a

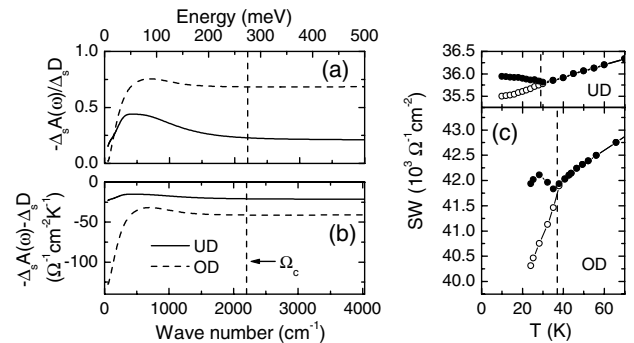


FIG. 4. The demonstration of the FGT sum rule violation in LSCO: (a) the relative finite-frequency SW, $-\Delta_s A(\omega)/\Delta_s D$; (b) absolute SW, $-\Delta_s A(\omega) - \Delta_s D$; (c) the temperature dependence of $A(\Omega_c)$ (open circles) and $A(\Omega_c) + D$ (solid circles). T_c is marked by the vertical line.

037004-3

mean-field treatment of the t - J model. One of them, a so-called ϕ gauge mode, acquires a weak c -axis spectral weight in the low-temperature orthorhombic structure due to the coupling to the buckling phonon mode. The energy scale of this mode is the in-plane exchange J (~ 100 – 150 meV), which agrees well with our observation.

The sum-rule analysis can be applied to $\Delta_s\sigma_1$ in the same manner as to $\Delta\sigma_1$. However, it directly relates to the usual FGT sum rule only close to T_c but not automatically for $T \ll T_c$. Figure 4(a) shows the relative SW, $-\Delta_s A(\omega)/\Delta_s D$. It saturates above Ω_c at the level of ~ 0.2 for $x = 0.12$ and ~ 0.7 for $x = 0.15$, thus clearly showing the presence of the FGT sum rule violation for both doping levels with relative values of almost 80% for the UD sample and 30% for the OD sample. This is in excellent agreement with the doping dependence found in YBCO [6]. In contrast to the relative violation, which is stronger in the UD sample, the absolute increase of the spectral weight $A(\Omega_c) + D$ below T_c is about 2 times larger for $x = 0.15$ [Fig. 4(b)]. This can also be directly deduced from Fig. 3(c) using formula (5). Thus the c -axis KE lowering is likely to be larger for the OD sample, which agrees with the prediction of Ref. [8]. The positive $\Delta_s\sigma_1$ at higher frequencies significantly increases the violation. Moreover, the ratio between the positive part of SW above the gap of the two doping levels [~ 2 ; see inset in Fig. 3(a)] is close to the ratio of $\Delta_s[A(\Omega_c) + D]$, which might indicate that the FGT sum rule violation is strongly related to the aforementioned collective mode. Finally, we plot the temperature dependence of $A(\Omega_c)$ and $A(\Omega_c) + D$ [Fig. 4(b)]. In the normal state the SW decreases with cooling down, which has to be taken into account for a proper formulation of the FGT sum rule. Below T_c $A(\Omega_c)$ starts to decrease faster as a result of the gap opening. The growth of $A(\Omega_c) + D$ in the SC state is a signature of the FGT sum rule violation.

In conclusion, our study, based on the combination of reflection and transmission spectra, reveals a detailed picture of the changes to the spectral weight in LSCO below T_c for energies up to 1.8 eV. The transition to the superconducting state is accompanied not only by the gap opening at low frequencies ($2\Delta \sim 20$ – 30 meV) but also by the increase of $\sigma_1(\omega)$ at higher energies up to 270 meV. The latter is interpreted as a possible occurrence of a new collective mode. Its origin is not yet established. The total low-frequency SW (including condensate) increases below T_c ; the absolute value of this growth is higher in the OD state, even though the relative FGT sum rule violation is much larger for the UD sample. Taking into account the new collective mode is decisive for a quantitative understanding of the implications of the sum rule violation. Our results match qualitatively several findings in YBCO, thus giving a hope that many of the “ c -axis effects” can be understood on the same basis in different cuprates in spite of a diversity of their crystal structures.

This investigation was supported by the Netherlands Foundation for Fundamental Research on Matter (FOM) with financial aid from the Nederlandse Organisatie voor Wetenschappelijk Onderzoek (NWO) and by DFG via SFB 608.

-
- [1] P.W. Anderson, *Science* **268**, 1154 (1995).
 - [2] D. Munzar *et al.*, *Phys. Rev. B* **64**, 024523 (2001).
 - [3] J. Schützmann *et al.*, *Phys. Rev. B* **55**, 11 118 (1997).
 - [4] K. A. Moler *et al.*, *Science* **279**, 1193 (1998); A. Tsvetkov *et al.*, *Nature (London)* **395**, 360 (1998).
 - [5] M. Tinkham and R. A. Ferrell, *Phys. Rev. Lett.* **2**, 331 (1959).
 - [6] D. N. Basov *et al.*, *Phys. Rev. B* **63**, 134514 (2001).
 - [7] D. N. Basov *et al.*, *Science* **283**, 49 (1999).
 - [8] J. E. Hirsch and F. Marsiglio, *Phys. Rev. B* **62**, 15 131 (2000).
 - [9] L. B. Ioffe and A. J. Millis, *Science* **285**, 1241 (1999).
 - [10] S. Uchida, K. Tamasaku, and S. Tajima, *Phys. Rev. B* **53**, 14 558 (1996).
 - [11] Y. Nakamura and S. Uchida, *Phys. Rev. B* **47**, 8369 (1993).
 - [12] D. N. Basov *et al.*, *Phys. Rev. B* **52**, R13 141 (1995).
 - [13] K. Tamasaku *et al.*, *Phys. Rev. Lett.* **72**, 3088 (1994).
 - [14] Because of the limited thermal contact of the thin sample with the holder the lowest sample temperature in the transmission experiment was 10 K for $x = 0.12$ and as high as 24 K for $x = 0.15$. It was calibrated by a comparison of the Josephson plasma edge in the spectra of R and T .
 - [15] Technically it is done by modeling $\epsilon(\omega)$ with a large number of oscillators (necessary to reproduce experimental data), including the zero-frequency lossless mode of the SC condensate.
 - [16] The samples are slightly wedged, which suppresses the Fabry-Pérot fringes. To account for this effect we introduced the rectangular thickness distribution with a width as an extra parameter. In this approximation the interference pattern was reproduced quite well, giving the thickness spreads of $0.5 \mu\text{m}$ for $x = 0.12$ and $1.5 \mu\text{m}$ for $x = 0.15$.
 - [17] M. Arai *et al.*, *Physica (Amsterdam)* **219–220B**, 225 (1996).
 - [18] This formula follows from the KK relation $\Delta_s\epsilon_1(\omega) = 8 \int_0^\infty \Delta_s\sigma_1(x)(x^2 - \omega^2)^{-1} dx$ assuming $\Delta_s\sigma_1(x > \Omega_c) = 0$. Although the FGT sum rule violation dictates that $\Delta_s\sigma_1(x) \neq 0$ at very high energies, the latter is very small up to at least 1.8 eV.
 - [19] W. Zimmermann *et al.*, *Physica (Amsterdam)* **183C**, 99 (1991).
 - [20] T. Nakano *et al.*, *J. Phys. Soc. Jpn.* **67**, 2622 (1998).
 - [21] D. Munzar *et al.*, *Solid State Commun.* **112**, 365 (1999).
 - [22] M. Grüninger *et al.*, *Phys. Rev. Lett.* **84**, 1575 (2000).
 - [23] C. C. Homes *et al.*, *Physica (Amsterdam)* **254C**, 265 (1995).
 - [24] P. A. Lee and N. Nagaosa, cond-mat/0211699.